Journal of Magnetism and Magnetic Materials 395 (2015) 234–239

Contents lists available at ScienceDirect

Journal of Magnetism and Magnetic Materials

journal homepage: www.elsevier.com/locate/jmmm

The role of magnetism in the formation of the two-phase miscibility gap in β Cu–Al–Mn

Fernando Lanzini [a,b,*], Alejandro Alés [a,b]

[a] Instituto de Física de Materiales Tandil (IFIMAT), Universidad Nacional del Centro de la Provincia de Buenos Aires (UNCPBA), Pinto 399, 7000 Tandil, Argentina

[b] Consejo Nacional de Investigaciones Científicas y Técnicas (CONICET), Argentina

ARTICLE INFO

Article history:
Received 2 February 2015
Received in revised form
6 July 2015
Accepted 24 July 2015
Available online 26 July 2015

Keywords:
Heusler alloys
Structural properties
Phase separation
Magnetic properties
DFT calculations

ABSTRACT

A theoretical study of the ground state properties of alloys with compositions along the pseudobinary line Cu_3Al–Cu_2AlMn is presented. Cohesive energies, lattice parameters and magnetic moments of the two limiting compounds and three intermediate compositions are calculated by means of density functional theory. In order to evaluate the role of magnetism, both the spin-polarized (SP) and the non spin-polarized (NSP) cases have been considered. It is shown that magnetism plays a central role on the stabilization of the $L2_1$ crystal structure in Cu_2AlMn, and in the formation of the miscibility gap in Cu_3Al–Cu_2AlMn. The considerable lattice mismatch between the end compounds can be attributed also to magnetic effects.

1. Introduction

The ternary Cu–Al–Mn system is a Hume-Rothery compound, for which the stability of different phases is determined by the conduction electron to atom ratio, e/a. For $e/a \approx 1.5$, the alloy displays a bcc (body centered cubic) based structure. As in other Cu-based shape memory alloys, the bcc β phase deserves interest from both the fundamental and applied points of view [1,2].

The experimental phase diagram is characterized by a wide miscibility gap (Fig. 1) between a DO_3 structure with composition close to Cu_3Al, and a $L2_1$ phase near the stoichiometric Heusler composition, Cu_2AlMn. These structures are described in Fig. 2. While Cu_3Al does not show magnetic properties, Cu_2AlMn exhibits a transition from a paramagnetic (pm) to a ferromagnetic (fm) configuration. This transition takes place at a Curie temperature (T_C) ranging from 590 to 641 K [3–6]. The spread of the experimental values for the Curie temperature can be mainly attributed to variations in the atomic (chemical) ordering [5,7–9] which, in turns, depends on the thermal history. Magnetic properties are due to magnetic moments of $\sim 4\,\mu_B$, localized at the Mn sites [10,11]. The coexistence between a paramagnetic and a ferromagnetic structure gives rise to interesting phenomena such as giant magnetoresistance [12,13] and superparamagnetism [14]. Despite the fact that the two phase region is well known to the experimentalists [15], the fundamental reasons behind such behavior are not completely understood. Three possible driving forces of the phase separation have been suggested: lattice mismatch effects, atomic ordering, and/or magnetic ordering. Marcos et al. [16] performed model Monte Carlo simulations and showed that, for certain values of the chemical and magnetic pair interactions, the interplay between chemical and magnetic ordering tendencies may give rise to the phase separation between a paramagnetic and a ferromagnetic ordered phases. In the experimental work of Kainuma et al. [3] it is suggested, instead, that the main reason for the formation of the miscibility gap is the lattice mismatch effect, arising from the considerable difference (~2%) in the lattice parameters of Cu_3Al and Cu_2AlMn.

In this work, a first-principles approach to this question is made. In particular, our main aim is to analyze the extent in which the magnetic properties influence the relative phase stability. Five ordered compounds along the pseudobinary line $Cu_3Al \leftrightarrow Cu_2AlMn$ (compositions $Cu_{3-x}AlMn_x$) are studied. Equilibrium lattice parameters, cohesive energies and magnetic moments are calculated. The rest of this paper is structured as follows: in Section 2 the methodology used in the calculations is introduced. In Section 3 the results of our calculations are presented and discussed; this section is subdivided into three parts. First, we briefly examine the role played by the magnetic interactions in determining the stability of the $L2_1$ structure in the Heusler compound Cu_2AlMn. The structural and magnetic properties of compounds with compositions $Cu_{3-x}AlMn_x$ are presented in Section 3.2. In the final subsection, the origin of

* Corresponding author at: Instituto de Física de Materiales Tandil (IFIMAT), Universidad Nacional del Centro de la Provincia de Buenos Aires (UNCPBA), Pinto 399, 7000 Tandil, Argentina.
E-mail address: flanzini@exa.unicen.edu.ar (F. Lanzini).

http://dx.doi.org/10.1016/j.jmmm.2015.07.068
0304-8853/

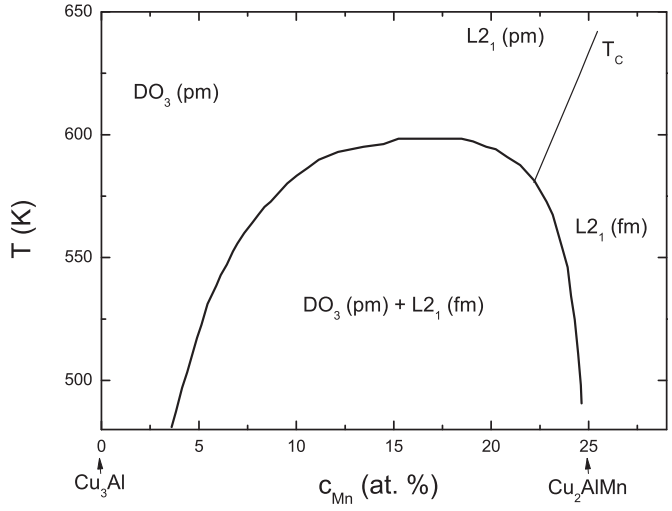

Fig. 1. Low temperature phase diagram of bcc Cu–Al–Mn along the pseudobinary $Cu_3Al \leftrightarrow Cu_2AlMn$ line ($e/a = 1.5$). Adapted from Ref. [3].

magnetism is discussed by analyzing the total and projected density of states (DOS) of the compounds. Finally, in Section 4 we outline the main conclusions of this work.

2. Methodology

Calculations of the electronic properties were performed using the PWscf code, distributed with the Quantum Espresso open-source package [17]. This is an integrated suite of computer codes, based on density functional theory (DFT) [18], plane waves, and pseudopotentials. In the present work, the atoms were represented by means of ultrasoft pseudopotentials [19], and the exchange correlation term by the Perdew–Burke–Erzenhorf [20] implementation of the Generalized Gradient Approximation.

Prior to the calculations, a careful examination of the energy convergence respect to different control parameters was performed. The energy cut-off for the plane wave expansion was established in 40 Ry, and for the charge density in 400 Ry. A uniform mesh of $10 \times 10 \times 10$ $\vec{k}$ points, automatically generated according to a Monkhorst-Pack scheme [21] was employed. The convergence criteria in the total energy for the self-consistent calculations was set to 1×10^{-8} Ry.

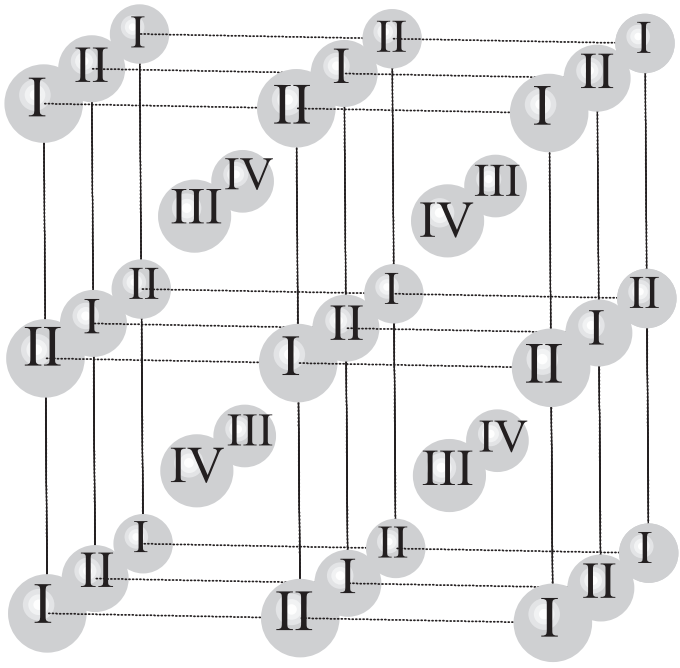

Fig. 2. Bcc lattice and the four interpenetrating fcc sublattices in which it is subdivided. In Cu_3Al with DO_3 structure, Cu atoms occupy sites I–III, and Al the sublattice IV; in $L2_1$ Cu_2AlMn, the sites III are occupied by Mn atoms.

Five ordered compounds along the line $Cu_{3-x}AlMn_x$ ($0 \le x \le 1$) were considered. Besides the limiting Cu_3Al with DO_3 configuration and Cu_2AlMn with $L2_1$ (and F43m) order, three ordered compounds with compositions $Cu_{11}Al_4Mn_1$, $Cu_{10}Al_4Mn_2$ and $Cu_9Al_4Mn_3$ were studied. These three intermediate systems, with 16 atoms per unit cell, were constructed starting from DO_3 Cu_3Al and replacing, respectively, 1, 2 or 3 Cu atoms in the sublattice III (Fig. 2) by Mn atoms. The corresponding compositions lie equidistantly between Cu_3Al and Cu_2AlMn. By construction, the obtained compounds can be seen as partially ordered $L2_1$; the lack of perfect order is due to non-stoichiometric compositions.

For each of the studied alloys, a structural optimization varying the cubic lattice parameter was done. The equilibrium state was determined by locating the minimum of the energy as a function of the lattice parameter, fitting the calculated data with a Murnaghan equation of state [22]. In order to quantify the effects of magnetism in the stability of the compounds, the optimization was performed in both the spin-polarized (SP) and non-spin-polarized (NSP) cases. For the SP calculations it has been assumed that the magnetic moments are due solely to Mn atoms, since, as we observed in preliminary calculations, and as noted also by other authors [23,24], magnetic contributions from other atoms are negligible.

3. Results

3.1. Equilibrium configuration of Cu_2AlMn

The Heusler compound Cu_2AlMn is the prototypical example of an $L2_1$ crystal [25], and its ferromagnetic behavior is known since 1903 [26]. In this work, in order to determine the relevance of the magnetic interactions on stabilizing the $L2_1$ phase, we analyzed the energetics of the alloy as a function of the lattice parameter and the magnetic state. For comparative purposes, we repeated the calculations for an F43m (Hg_2CuTi- type) structure. This is other simple structure ordered in first and second neighbors, and has been found to be the ground state configuration in the related Mn_2CuAl alloy [27,28]. Thus, this is a possible competing phase for the $L2_1$ structure. The F43m structure can be defined with the help of Fig. 2: Cu atoms occupy sublattices I and III, Mn is placed in II, and Al in IV.

The variation of the electronic energy with the lattice parameter in Cu_2AlMn is displayed in Fig. 3. Calculations were done for the $L2_1$ and F43m atomic distributions for both the SP and the NSP cases. It is appreciable from the figure that in the NSP calculations, the F43m structure is predicted to be energetically favorable over the $L2_1$; the difference between both minima, located at almost the same lattice parameter, is 1.58 mRy. Inclusion of magnetism leads to dilatation of the lattice and, interestingly, to an inversion of the relative stabilities. The well-known ferromagnetic $L2_1$ phase is now correctly predicted as the ground state configuration, with a difference in energy of 4.8 mRy respect to the F43m structure.

3.2. $Cu_{3-x}AlMn_x$ line

The formation energies, equilibrium lattice parameters and magnetic moments of five compounds belonging to the pseudobinary $Cu_{3-x}AlMn_x$ line are listed in Table 1, for both SP and NSP calculations.

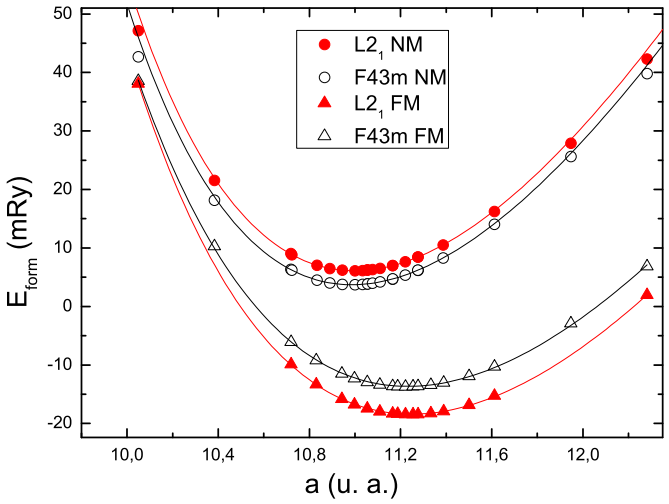

Fig. 3. Formation energy as a function of the lattice parameter for Cu_2AlMn with atomic configuration $L2_1$ (full symbols) and F43m (open symbols). Triangles correspond to spin-polarized (SP), and circles to non spin-polarized (NSP) calculations. The lines through the data are Murnaghan fits.

Table 1
Equilibrium lattice parameter, formation energies and magnetic moments (per Mn atom) of five compounds with composition $Cu_{3-x}AlMn_x$.

		NSP calculations		SP calculations		
x	Stoichiometry	a (u. a.)	E_{form} (mRy)	a (u. a.)	μ (μ_B)	E_{form} (mRy)
0	Cu_3Al	11.074	−17.1	11.074	–	−17.1
0.25	$Cu_{11}Al_4Mn_1$	11.015	−12.1	11.123	3.46	−16.5
0.5	$Cu_{10}Al_4Mn_2$	11.038	−6.2	11.172	3.60	−16.4
0.75	$Cu_9Al_4Mn_3$	11.052	−0.3	11.216	3.66	−17.0
1	Cu_2AlMn	10.997	+6.1	11.248	3.63	−18.4

The formation energy of a compound $Cu_xAl_yMn_z$ is calculated as the difference of the electronic energy per atom of the compound and that of the pure elements:

$$E_{\text{form}}(Cu_xAl_yMn_z) = E(Cu_xAl_yMn_z) - \frac{xE(Cu) + yE(Al) + zE(Mn)}{x + y + z}$$

with $E(A)$ the energy per atom of the element A. We have taken as reference states for pure Cu and Al the bcc non-magnetic structures with minimum electronic energy, which corresponds, respectively, to lattice parameters $a_{Cu}=5.456$ a u, and $a_{Al}=6.140$ a u. These values are in agreement with those reported in previous works using different ab-initio methodologies [29–32]. For pure

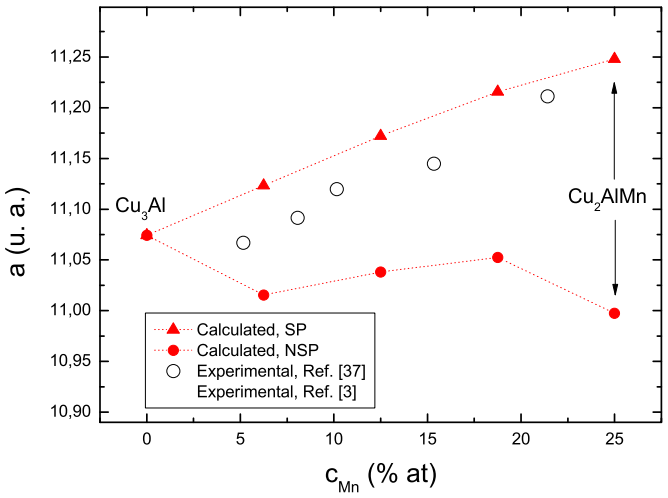

Fig. 5. Equilibrium lattice parameters for alloys along the $Cu_3Al \leftrightarrow Cu_2AlMn$ line.

Mn with bcc structure, we have found the ground state to be antiferromagnetic (in particular, the configuration AFM II discussed by Sliwko et al. [33]) with $a_{Mn}=5.51$ a u. This value is in the range of the ones calculated by other authors [34–36].

The formation energies of the structures listed in Table 1 are plotted against Mn content in Fig. 4a and b for the NSP and SP calculations, respectively. In the NSP case, the formation energies of the intermediate compounds lie below the line connecting the end structures Cu_3Al and Cu_2AlMn. This means that the intermediate, non-stoichiometric compounds, are predicted to be energetically favorable over the mixture Cu_3Al+Cu_2AlMn, and thus are predicted as stable against phase decomposition. This is clearly contrary to the experimental evidence. On the other hand, in the SP calculations (Fig. 4b), the formation energies of the intermediate compounds lie above the tie-line connecting the end points. This indicate that the intermediate, partially ordered compounds, are unstable against decomposition in the two phase field, in agreement with the experiment. These results highlight the fundamental role played by magnetism in the phase separation.

The calculated lattice parameters are confronted with the experimental data [3,37] in Fig. 5. The results of the SP DFT calculations approximately follow a Vegard's law, in the sense that the lattice parameter of the alloys increases almost linearly with the Mn content. The SP results show a good agreement with the experimental values. On the other hand, the NSP calculations lead to an underestimation of the lattice constant and a more complicated

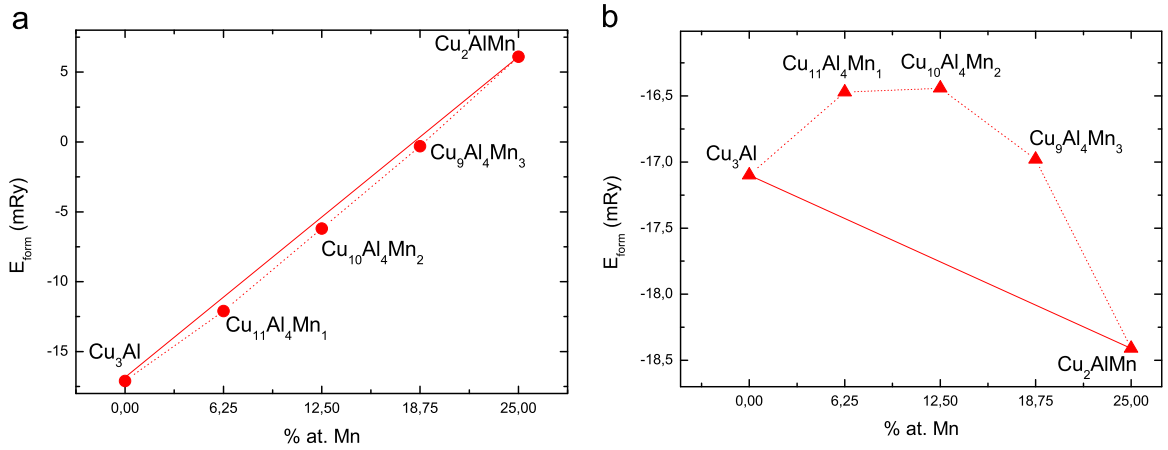

Fig. 4. Cohesive energies for compounds along the $Cu_{3-x}AlMn_x$ line: (a) NSP and (b) SP calculations.

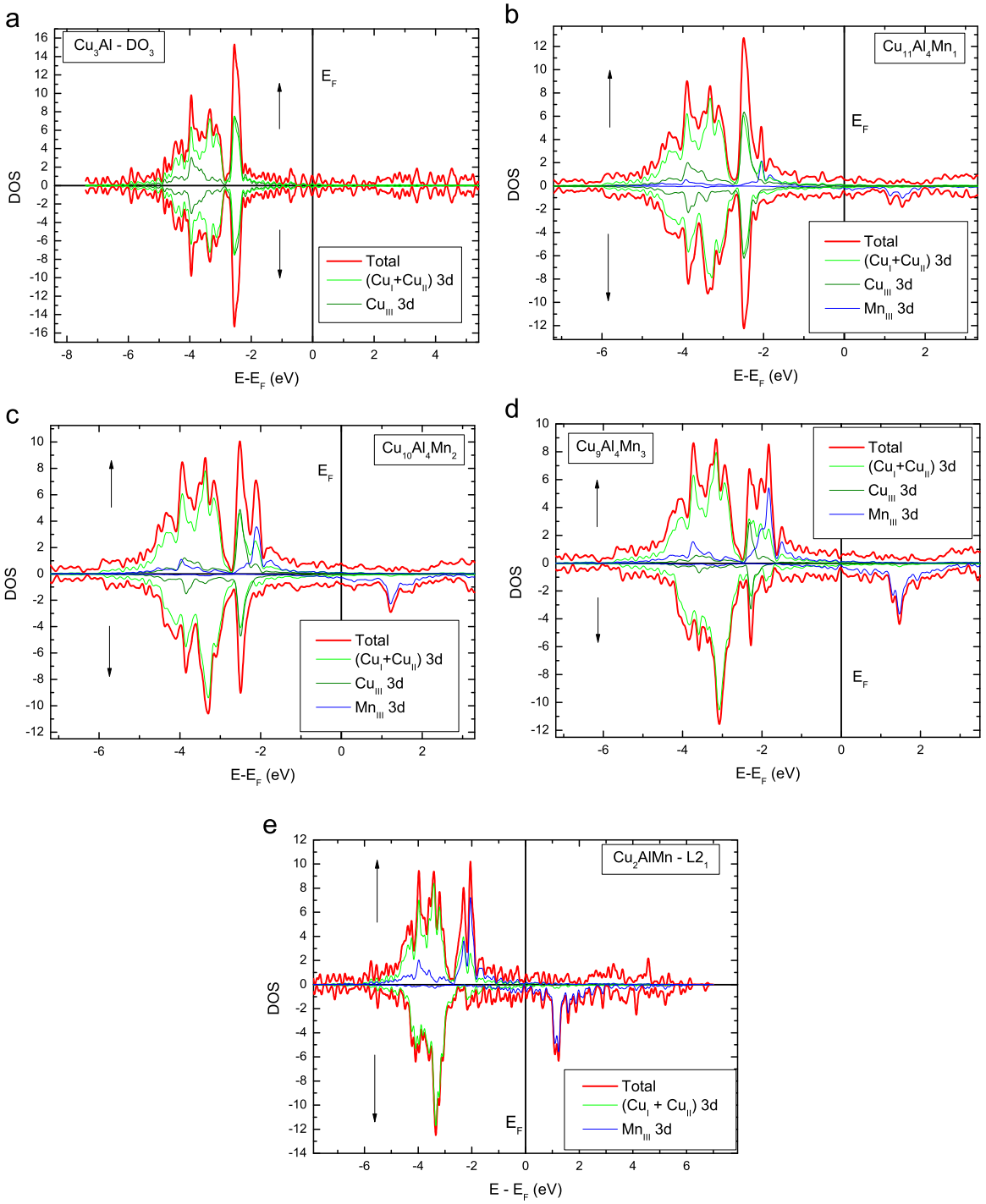

Fig. 6. Total and projected DOS of five compounds with composition $Cu_{3-x}AlMn_x$. (a) Cu_3Al; (b) $Cu_{11}Al_4Mn_1$; (c) $Cu_{10}Al_4Mn_2$; (d) $Cu_9Al_4Mn_3$; (e) Cu_2AlMn.

variation as a function of the Mn content. The fact that the SP equilibrium lattice parameters for the alloys containing Mn are higher than the ones corresponding to the NSP case is related to the general trend observed in transition metals that the magnetic states are favored at large volumes, and the non-magnetic states are favored at low volumes [34]. Experimentally, the lattice parameter of $L2_1$ Cu_2AlMn is about 2% larger than the one of DO_3 Cu_3Al. This lattice mismatch has been suggested as one of the driving forces behind the phase separation [3]; Fig. 5 shows that this difference in lattice parameters cannot be explained without considering magnetic effects.

Table 1 also shows that the magnetic moment (per Mn atom) remains almost unchanged independently of the relative content of magnetic atoms. This issue will be discussed in the next Subsection.

3.3. Total and partial density of sates

The total and projected electronic density of states (DOS) for the five compounds of interest are shown in Fig. 6. In all the cases, the upper half of the figure represent the majority spin contribution, and the lower half that of the minority spin states; the thinner lines are the contributions of *d* states, and we separate the

ones coming from Cu atoms in the equivalent sites I and II, and Cu or Mn atoms in sites III (Fig. 2).

The DOS of DO_3 Cu_3Al is completely symmetric for the 'majority' and 'minority' spin directions, consistently with the absence of a magnetic moment. The structure is characterized by a double peak: a narrow peak at ~2.5 eV below the Fermi level (antibonding states), and a second, broader peak (bonding states), in the range from −2.8 to −5 eV. The replacement of one of the Cu_{III} by Mn ($Cu_{11}Al_4Mn_1$ composition) leads to a drastic modification in the DOS. It is seen that, while the Mn majority-spins join with the Cu *d* electrons to form a common valence *d* band, the minority-spins are displaced to the conduction band, with a peak in the region 1–2 eV above the Fermi level. Thus, whereas the Mn majority-spin states are almost completely occupied, the minority-spin states are almost completely emptied. This exchange splitting in the DOS of Mn leads to a net magnetic moment of 3.46 μ_B (see Table 1). Increasing further the Mn content (compositions $Cu_{10}Al_4Mn_2$ and $Cu_9Al_4Mn_3$) leads to quantitative, but not qualitative, changes in the DOS. As Cu is replaced by Mn, the antibonding peak in the minority-spin total DOS, which in Cu_3Al is placed well below the Fermi level, gradually decreases in size, while the Mn peak in the conduction band increases. The magnetic moment per Mn atom is not substantially modified. The DOS for Cu_2AlMn has been calculated and extensively discussed by other authors [23,38]. Our results agree with these previous calculations: Cu 3d states for majority- and minority-spins are located in the 2–6 eV region of the valence band, and the main contribution of the Mn 3d majority-spin is around 2 eV in the valence band. Most of the Mn 3d minority-spin orbital are located within 3 eV above the Fermi level.

The calculated magnetic moment for the unitary cell of Cu_2AlMn is 3.63 μ_B. This value is somewhat higher than former theoretical estimates (3.38 μ_B[38] and 3.20–3.40 μ_B[23]) but agrees well with more recent DFT calculations (3.60 μ_B in [39], 3.59 μ_B [27]). The small discrepancy with these last results can be attributed to the use of different computational implementations (basis set for the wave functions, pseudopotentials, control parameters of the self-consistent calculation). The reported experimental values of the magnetic moment range between 3.1 and 4.12 μ_B [4,7,11,24,40,41]; the spread can be attributed to variations in experimental conditions, such as the measurement temperature or small deviations from the stoichiometric composition. For instance, measurements by Feng et al. [42] show that a small Mn excess leads to a notorious decrement of the magnetic moment. However, it is interesting to note that the careful extrapolation to $T=0$ K performed by Endo et al. [41] gives $\mu=(3.61\pm0.04)$ μ_B; our result lies within this range.

4. Conclusions

In this work, we analyzed the role played by magnetism on the stability of different compounds with compositions along the pseudo-binary line $Cu_{3-x}AlMn_x$.

First, we examined the influence of magnetism on the stabilization of the crystalline structure $L2_1$ in Cu_2AlMn. We have found that, when the magnetism is not taken into consideration, DFT calculations predict that the F43m phase is energetically more stable than the $L2_1$ one. When the possibility of magnetism is included through the use of spin polarized calculations, the trend is reversed, and the ferromagnetic $L2_1$ phase is correctly predicted as stable. Although this is beyond the purposes of the present work, it will be interesting to check if this behavior is also observed in other magnetic Heusler compounds.

The phase separation DO_3–Cu_3Al+$L2_1$–Cu_2AlMn, observed experimentally at low temperatures, can be explained in terms of magnetic effects only. If the possibility of magnetism is excluded, intermediate compounds with partial order are predicted to be stable against this phase decomposition. On the other hand, when the Mn-containing compounds are assumed to be ferromagnetic, such intermediate compounds are correctly predicted as unstable.

The equilibrium lattice parameters obtained in the SP calculations increases linearly with the Mn content, in agreement with experimental determinations. The calculated relative difference in lattice parameter for the end compounds Cu_3Al and Cu_2AlMn is 1.86% (the experimental value is ~2% [3]). This lattice mismatch has been suggested to be the main driving force of the phase decomposition. Here we showed that, in turns, this difference in lattice parameters has a magnetic origin, since NSP calculations predict a completely different variation of the lattice parameter with the Mn content.

The magnetic moments (per magnetic atom) of all the Mn-containing compounds are in the range 3.46–3.66 μ_B, i. e., it does not seem to be sensitive to the relative content of Cu and Mn. The analysis of the total and projected DOS indicates that the mechanism of formation of the magnetic moments is analogous in all the compounds of interest: the majority-spin *d* electrons of Mn form a common band with those of Cu, whereas the minority-spin *d* Mn states locate above the Fermi level. The independence of the magnetic moment on the Cu content is consistent with the more general analysis of Kübler et al. [38] according to which, in Heusler X_2MnY alloys, the main role of *X* atoms is the determination of the lattice parameter (see Fig. 5), whereas the *Y* atoms provide the *p* orbitals that mediate the coupling of the magnetic moments localized at the Mn sites.

Acknowledgments

This work was financially supported by ANPYCT (PICT 2012-0868), CONICET, SECAT-UNCPBA and CICPBA.

References

[1] T. Tadaki., Cu-based shape memory alloys, in: K. Otsuka, C.M. Wayman (Eds.), Shape Memory Materials, Cambridge University Press, UK, 1998.
[2] L. Delaey, Diffusionless Transformations, in: P. Haasen (Ed.), Materials Science and Technology, vol 5: Phase Transformation in Materials, VCH, Weinheim, 1991.
[3] R. Kainuma, N. Satoh, X.J. Liu, I. Ohnuma, K. Ishida, J. Alloy. Compd. **266** (1998) 191.
[4] D.P. Oxley, R.S. Tebble, K.C. Williams, J. Appl. Phys. 34 (1963) 1362.
[5] Y.V. Kudryavtsev, V.A. Oksenenko, N.N. Lee, Y.P. Lee, J.Y. Rhee, J. Dubowic, J. Appl. Phys. **97** (2005) 113903.
[6] B. Dubois, D. Chevereau, J. Mater. Sci. 14 (1979) 2296.
[7] G.B. Johnston, E.O. Hall, J. Phys. Chem. Solids 29 (1968) 193.
[8] R. Winkler, E. Wachtel, J. Magn. Magn. Mater. 9 (1978) 270.
[9] A. Alés, F. Lanzini, Model. Simul. Mater. Sci. Eng. 22 (2014) 085007.
[10] Y. Ishikawa, Physica B+C 91 (1977) 130.
[11] K. Tajima, Y. Ishikawa, P.J. Webster, M.W. Stringfellow, D. Tocchetti, K.R. A. Ziebeck, J. Phys. Soc. Jpn. 43 (1977) 483.
[12] L. Yiping, A. Murthy, G.C. Hadjipanayis, H. Wang., Phys. Rev. B 54 (1996) 3033.
[13] M. Zhang, G. Liu, Y. Cui, H. Hu, Z. Liu, J. Chen, G. Wu, Y. Sui, Z. Qian, X. Zhang, J. Magn. Magn. Mater. 278 (2004) 328.
[14] T.V. Yefimova, V.V. Kokorin, V.V. Polotnyuk, A.D. Shevchenko, Phys. Met. Metallogr. 64 (1987) 189.
[15] M. Bouchard, G. Thomas, Acta Metall. 23 (1975) 1485.
[16] J. Marcos, E. Vives, T. Castán, Phys. Rev. B 63 (2001) 224418.
[17] P. Giannozzi, et al., J. Phys.: Condens. Matter 21 (2009) 395502.
[18] (a) P. Hohenberg, W. Kohn., Phys. Rev. 136 (1964) B864;
(b) W. Kohn, L.J. Sham, Phys. Rev. 140 (1965) A1133.
[19] D. Vanderbilt, Phys. Rev. B 41 (1990) 7892.
[20] J.P. Perdew, K. Burke, M. Ernzerhof, Phys. Rev. Lett. 77 (1996) 3865.
[21] H.J. Monkhorst, J.D. Pack, Phys. Rev. B 13 (1976) 5188.
[22] F.D. Murnaghan, Proc. Natl. Acad. Sci. U. S. A. 30 (1944) 244.
[23] A. Deb, Y. Sakurai, J. Phys.: Condens. Matter 12 (2000) 2997.
[24] W. Zukowski, A. Andrejczuk, L. Dobrzynski, M.J. Cooper, M.A.G. Dixon, S. Gardelis, P.K. Lawson, T. Buslaps, S. Kaprzyk, K.U. Neumann, K.R.A. Ziebeck, J. Phys.: Condens. Matter 9 (1997) 10993.
[25] A.J. Bradley, J.W. Rodgers, Proc. R. Soc. Lond. A 144 (1934) 340.

[26] F. Heusler, Vehr. Deuts. Phys. Ges. 5 (1903) 219.
[27] S.T. Li, Z. Ren, X.H. Zhang, C.M. Cao, Physica B 404 (2009) 9651 404 (2009) 965.
[28] Z.Q. Feng, H.Z. Luo, Y.X. Wang, Y.X. Li, W. Zhu, G.H. Wu, F.B. Meng, Phys. Status Solidi A 207 (2010) 1481.
[29] J.Z. Liu, A. van de Walle, G. Ghosh, M. Asta, Phys. Rev. B 72 (2005) 144109.
[30] F. Jona, P.M. Marcus, Phys. Rev. B 63 (2001) 094113.
[31] F. Lanzini, P.H. Gargano, P.R. Alonso, G.H. Rubiolo, Modell. Simul. Mater. Sci. Eng. 19 (2011) 015008.
[32] P.G. Gonzales-Ormeño, H.M. Petrilli, C.G. Schön, Calphad 26 (2002) 573.
[33] V. Sliwko, L. Blaha, P. Mohn, K. Schwarz, Int. J. Mod. Phys. B 7 (1993) 614.
[34] V.L. Moruzzi, P.M. Marcus, P.C. Pattnaik, Phys. Rev. B 37 (1988) 8003.
[35] T. Asada, K. Terakura, Phys. Rev. B 47 (1993) 15992.
[36] J. Hafner, D. Hobbs, Phys. Rev. B 68 (2003) 14408.
[37] S. Sugimoto, S. Kondo, H. Nakamura, D. Book, Y. Wang, T. Kagotani, R. Kainuma, K. Ishida, M. Okada, M. Homma, J. Alloy. Compd. 265 (1998) 273.
[38] J. Kübler, A.R. Williams, C.B. Sommers, Phys. Rev. B 28 (1983) 1745.
[39] I. Galanakis, E. Şaşioğlu, J. Mater. Sci. 47 (2012) 7678–7685.
[40] L.D. Khoi, P. Veillet, I.A. Campbell, J. Phys. F: Metal Phys. 8 (1978) 1811–1824.
[41] K. Endo, T. Ohoyama, R. Kimura, J. Phys. Soc. Jpn. 17 (1964) 1494–1495.
[42] L. Feng, L. Ma, Z.Y. Zhu, W. Zhu, E.K. Liu, J.L. Chen, G.H. Wu, F.B. Meng, H.Y. Liu, H.Z. Luo, Y.X. Li, J. Appl. Phys. 107 (2010) 013913.